



IJRASET

International Journal For Research in
Applied Science and Engineering Technology



INTERNATIONAL JOURNAL FOR RESEARCH

IN APPLIED SCIENCE & ENGINEERING TECHNOLOGY

Volume: 5 Issue: XI Month of publication: November 2017

DOI:

www.ijraset.com

Call:  08813907089

E-mail ID: ijraset@gmail.com

Growth, Spectral, Optical and Nonlinear Optical Characterization of R- Mandelic Acid Single Crystals

K. Sivakumar¹, M. Senthilkumar², C. Ramachandra raja³

¹Department of Physics, Government Arts College (Autonomous), Kumbakonam- 612 002, India.

Abstract: In this work, single crystals of R-Mandelic Acid (RMA) are developed by low temperature solvent evaporation method. These crystals were characterized using several techniques. The lattice parameters were determined by X-ray diffraction analysis. FTIR and FT-Raman spectroscopy were employed to analyses the vibrations of functional groups. The cut-off wavelength and transmission region were measured by UV-Vis-NIR spectroscopy. Thermal behavior of the crystal was investigated by TG/DTA study. FT-NMR analysis was carried out to establish the molecular structure. Green light emission confirms the second harmonic generation of RMA. Negative nonlinearity and saturable absorption property of RMA were revealed by Z-scan test.

Keywords: Crystal Growth; XRD; Spectroscopy; Nonlinear optics; Z-scan.

I. INTRODUCTION

Nonlinear optical (NLO) crystals play vital role in several laser based devices. Nitrile combination is suitable and artificially important chemical building blocks because they are commonly used in the organic fusion of compounds such as amides, carboxylic acids and their derivatives. There is a considerable industrial interest in enzymatic conversion of various nitriles owing to the desirability of conducting such conversions under mild conditions that would not alter other labile reactive groups [1-4]. R-mandelic acid is a chiral building block for the presentation of anti obesity agents, antitumor agents, penicillins, semi synthetic cephalosporin's, etc., and it is also used as a chiral resolving agent. Production of R- mandelic acid can be achieved by chemical as well as by different enzymatic routes. Nitrifies mediated pathway offers significant advantages over other routes because of the absence of the cofactor involvement, cheap starting material in the form of mandelonitrile and above all a possibility of carrying out a dynamic kinetic resolution which provides theoretically 100% yield of R-(-) mandelic acid [5-6]. RMA is used in the X-ray spectroscopy as an analyzer. Its space group and crystal system are $P2_1$ and monoclinic respectively [7]. In the present work, crystals of RMA are grown using solution growth method. They were characterized by XRD analysis, UV-Vis-NIR spectroscopy, FT-IR, FT-Raman and FT-NMR spectroscopy. TG/DTA analysis, SHG test, Z-scan test and the observations are reported.

II. EXPERIMENTAL

A. Growth of R-Mandelic acid

RMA was developed by solvent evaporation method at 37°C using a constant temperature bath. RMA (6 g) was dissolved in 50 ml deionized water. This solution was stirred for 3 hours, and then the supersaturated solution was filtered by What man filter paper, after it was closed with a perforated cover. It was maintained at 37°C using constant temperature bath of accuracy $\pm 0.1^\circ\text{C}$. Then the seed crystals were harvested attain an well crystals and shape in time period of 25 days, optically transparent and good quality single crystals of RMA were grown at the bottom of the beaker. The photograph of the grown crystals are presented figure 1.

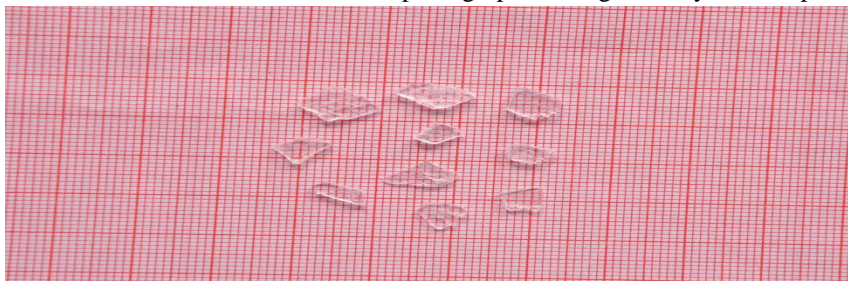


Fig.1 Photograph of RMA single crystals

B. Characterization

Single crystal X-ray diffraction study of RMA was carried out using Bruker AXS kappa Apex2 diffractometer. The powder XRD study was done by Ultima3 theta-theta gonio X-ray diffractometer. The transmission spectrum was recorded between 190 nm and 1100 nm. FTIR spectrum was recorded between 4000 cm^{-1} and 400 cm^{-1} by PERKIN ELMER RX1 spectrometer. FT-Raman spectrum was recorded between 4000 cm^{-1} and 50 cm^{-1} employing BRUKER: RFS 27 spectrometer. Thermal nature of the grown crystal was studied using TG/DTA analysis (SDT Q600 V20.9 Build 20). ^1H NMR and ^{13}C NMR spectra of RMA single crystals were recorded using Bruker FT-NMR spectrometer. The SHG efficiency was measured using a Q-switched, mode locked Nd:YAG laser. In the Z-scan study, the far field intensity is measured as a function of the sample position using 632.8 nm laser.

III. RESULT AND DISCUSSION

A. Single crystal XRD analysis

Well shaped, transparent and quality of RMA single crystal are subjected to single crystal XRD analysis at room temperature. This study shows that RMA crystallizes in monoclinic crystal system and the measured cell parameters are $a = 8.666 \pm 0.019 \text{ \AA}$, $b = 5.870 \pm 0.006 \text{ \AA}$, $c = 15.206 \pm 0.020 \text{ \AA}$; $\alpha = \gamma = 90^\circ$ $\beta = 102.87^\circ$, and the cell volume $V = 754 \pm 2 \text{ \AA}^3$. These results matches well with the results of Patil et al [7].

B. Powder XRD analysis

The powder XRD analysis was determined by a Rich-Seifert diffractometer with $\text{CuK}\alpha$ ($\lambda = 1.5406 \text{ \AA}$) radiation. The indexed powder XRD pattern of the grown crystal RMA is shown in Figure 2. The powdered RMA sample was scanned over the range $5^\circ - 80^\circ$ at the rate of 1° per min. The sharp and strong peaks are confirmed the good crystallinity of the grown crystal. From the powder X-ray data, the various planes of reflections (hkl) were indexed by indx software program. The obtained lattice parameters from the powder XRD analysis are in good agreement with the literature reported values and single crystal XRD analysis. The structural data for RMA single crystal and powder X-ray data are listed in Table 1.

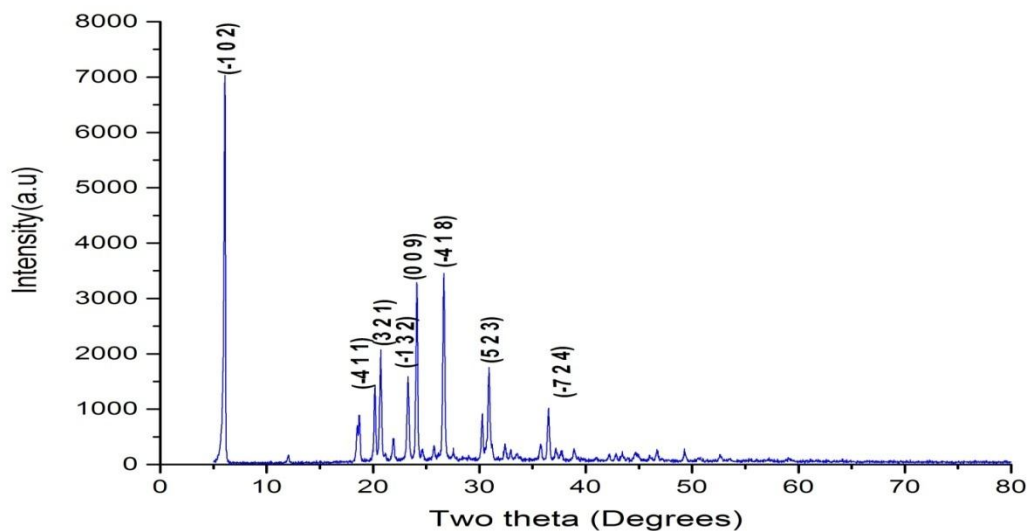


Fig.2. Powder XRD pattern of RMA crystal

Table 1. Comparison of crystal data of single crystal XRD and powder XRD

XRD Analysis	a(Å)	b (Å)	c (Å)	V (Å) ³
Single crystal XRD	8.666	5.870	15.206	754
Powder XRD	8.495	5.871	15.158	753

C. UV-Vis-NIR Analysis

The recorded transmission spectrum of RMA is given in Fig.3. RMA is transparent from 267 nm to 1100 nm. NLO crystals are mainly used in the frequency conversion of laser wavelengths. Harmonic generation, sum frequency generation, differential frequency generation, optical parametric oscillation are some of the NLO processes which are employed to convert fixed laser wavelength into other wavelengths. As RMA is transparent from 267 nm to 1100 nm, it can be effectively used to convert the fundamental of Nd: YAG wavelength (1064 nm) into its second harmonic (532 nm). RMA can also be effectively used to generate other wavelengths employing other NLO processes.

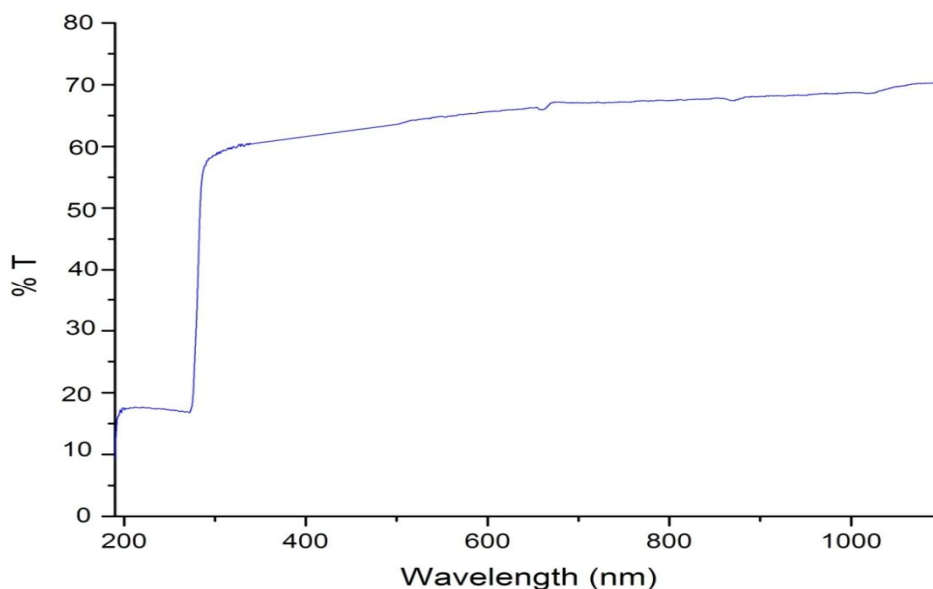


Fig. 3 UV-Vis-NIR spectrum of RMA crystal

D. FT-IR and FT-Raman spectral study of RMA

The FTIR and FT-Raman spectra are shown in Fig. 4 and Fig. 5 respectively. In FT-IR spectrum, the strong peak at 3450 cm^{-1} assigned to OH asymmetric stretching. In the FT-Raman spectrum, the peak observed around $3060, 2979, 2909\text{ cm}^{-1}$ assigned to C-H symmetric stretching and the same was observed in IR spectrum as a broad peak between 2900 cm^{-1} and 3036 cm^{-1} . The FT-IR band at 1959 cm^{-1} assigned to C-H out of plane bending. FTIR band present at 1722 cm^{-1} assigned to C=O stretching and the same was observed in Raman spectrum at 1712 cm^{-1} . The FT-Raman peak observed at 1603 cm^{-1} assigned to C=C stretching vibration. In FT-IR Spectrum, peak at 1495 cm^{-1} corresponds to OH symmetric stretching. The FT-IR band at 1455 cm^{-1} assigned to C-H symmetric stretching. FTIR band present at 1286 cm^{-1} corresponds to COOH stretching vibration and the same was observed in Raman spectrum at 1285 cm^{-1} . FTIR band present at 1193 cm^{-1} corresponds to C-O stretching vibration and the same was observed in Raman spectrum at 1178 cm^{-1} . FTIR band present at 1063 cm^{-1} corresponds to C-C stretching vibration and the same was observed in Raman spectrum at 1063 cm^{-1} . The FT-IR peak at 1026 cm^{-1} assigned to C=C stretching vibration The FT-IR peak at 1002 cm^{-1} assigned to C-C stretching vibration. FTIR band present at 934 cm^{-1} corresponds to C=O stretching and the same was observed in Raman spectrum at 933 cm^{-1} . FTIR band present at 862 cm^{-1} assigned to C=O stretching and the same were observed in Raman spectrum at 860 cm^{-1} . In FT-IR spectrum, the intense band at 835 cm^{-1} assigned to OH symmetric stretching. In IR spectrum peak at 769 cm^{-1} assigned to OH rocking vibration and the same was observed in Raman spectrum at 756 cm^{-1} . In IR spectrum, peak at 726 cm^{-1} assigned to C-H rocking vibration and the same was observed in Raman spectrum at 728 cm^{-1} . In the FT-IR spectrum, the peak at 693 cm^{-1} assigned to C-H stretching vibration. FTIR peak at 645 cm^{-1} assigned to COOH bending and the same was present in Raman spectrum at 643 cm^{-1} . The IR band at 495 cm^{-1} is due to COH rocking vibration and the same was present in Raman spectrum at 522 cm^{-1} . These assignments are listed in Table 2. The result matches with literature values [8-9]. As most of the vibrations are observed both in IR and Raman spectra, the crystal is noncentro symmetric in nature.

Table 2. FT-IR and FT-Raman assignments of RMA crystal

FTIR (cm ⁻¹)	FT-Raman (cm ⁻¹)	Assignments
3450	-	O-H asymmetric stretching
2900- 3036	3060, 2979, 2626	C-H asymmetric stretching
1959	-	C-H out of plane bending
1722	1712	C=O stretching vibration
-	1603	C=C stretching vibration
1495	-	O-H symmetric stretching
1455	-	C-H symmetric stretching
1286	1285	COOH stretching vibration
1193	1178	C-O stretching vibration
1063	1063	C-C stretching vibration
-	1026	C=C stretching vibration
-	1002	C-C stretching vibration
934	933	C=O stretching vibration
862	860	C=O stretching vibration
-	835	O-H symmetric stretching
769	756	O-H rocking vibration
726	728	C-H rocking vibration
645	643	COOH bending vibration
494	522	OH rocking vibration

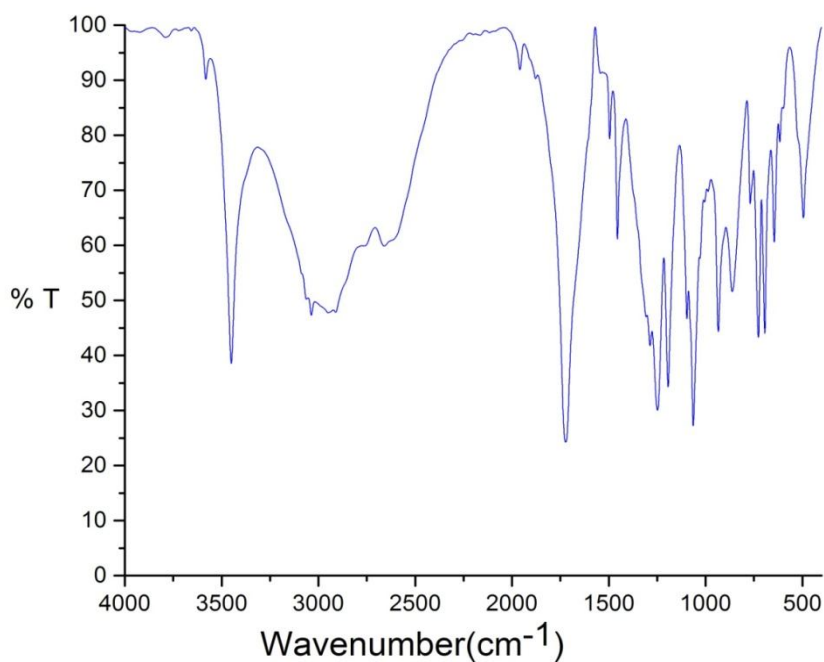


Fig.4. FT-IR spectrum of RMA crystal

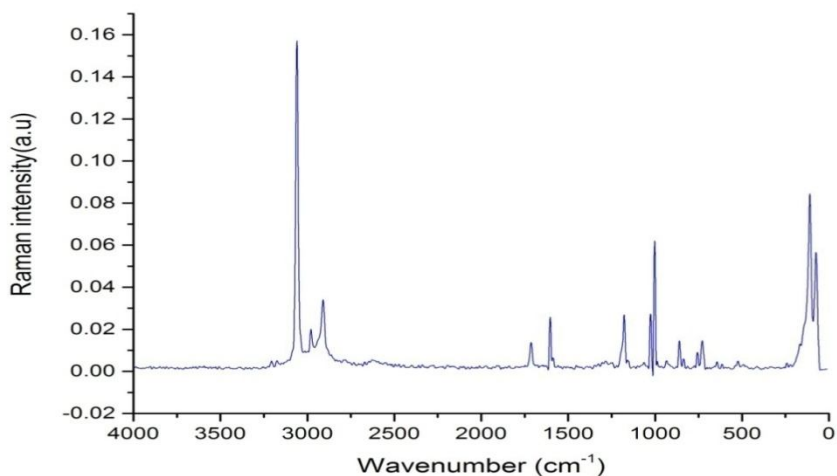


Fig.5. FT-Raman spectrum of RMA crystal

The thermograms of RMA is presented in fig.6 (a) and 6 (b). Initially, 4.614 mg of RMA was kept in a container. It was heated at a rate of 10 °C /min in nitrogen atmosphere. The TGA curve shows the thermal stability of the crystal up to 201°C. Between 201°C and 310°C, the crystal completely decomposes. The endothermic peak obtained at 137°C may correspond to the RMA melting temperature. Successive endothermic peaks correspond to the decomposition of the crystal.

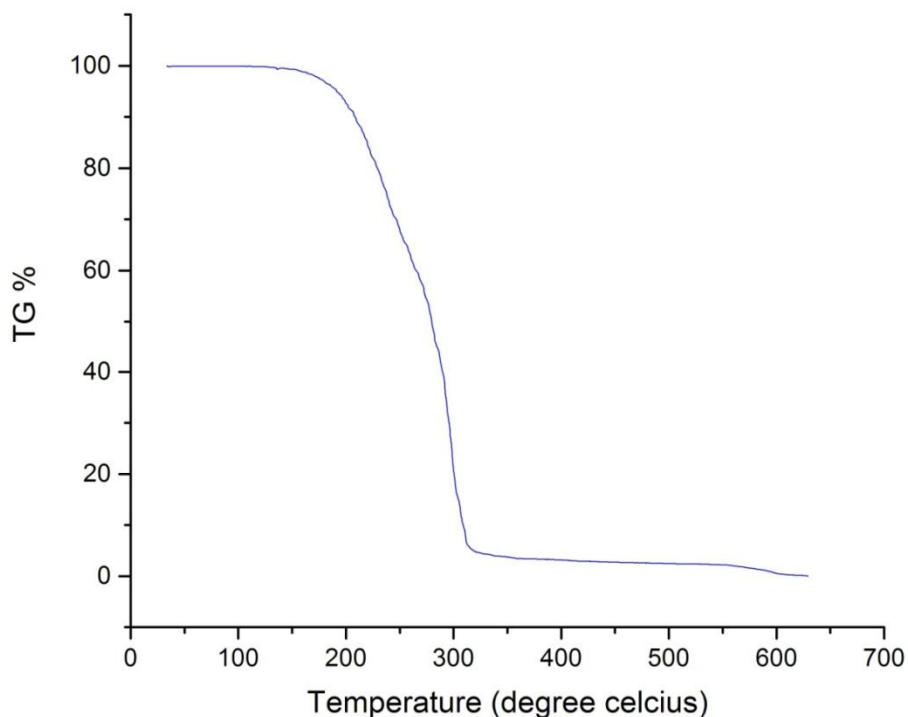


Fig.6. (a) TGA Curve of RMA crystal

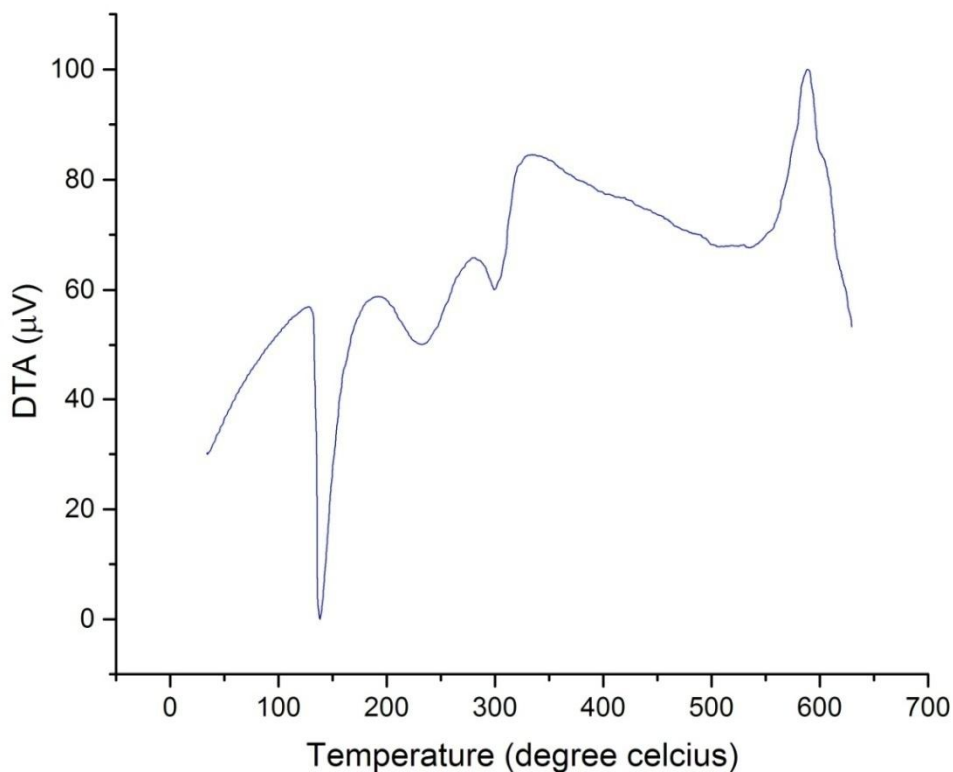


Fig.6. (b) DTA Curve of RMA crystal

G. NMR Studies

The ^1H NMR and ^{13}C NMR spectra of RMA are given in Fig. 8 and Fig.9 respectively. The chemical shifts and assignments are presented in Table 3. The ^1H NMR spectrum of RMA can be understood with the help of the molecular structure shown in Fig.7 (a) [10].

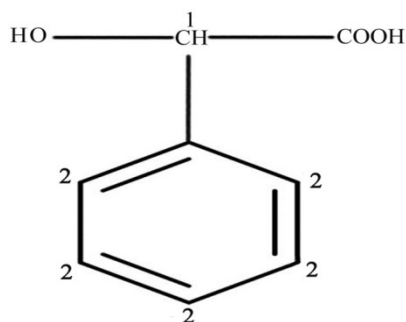


Fig.7 (a) ^1H NMR atomic numbering of RMA crystal

In ^1H NMR spectrum, signal due to racemic mandelic acid is observed at 7.359 ppm and 7.339 ppm and is assigned to CH proton of ring. The peak at 5.175 ppm is due to the proton present in 1 position. The strong intense solvent signal appeared at 4.702 ppm. The

absence of signals for OH and COOH protons indicates the deuterium exchange reaction in OH and COOH, when deuterium oxide was used as the solvent [11].

The ^{13}C NMR spectrum of RMA can be understood with the help of the molecular structure shown in Fig.7 (b) [10].

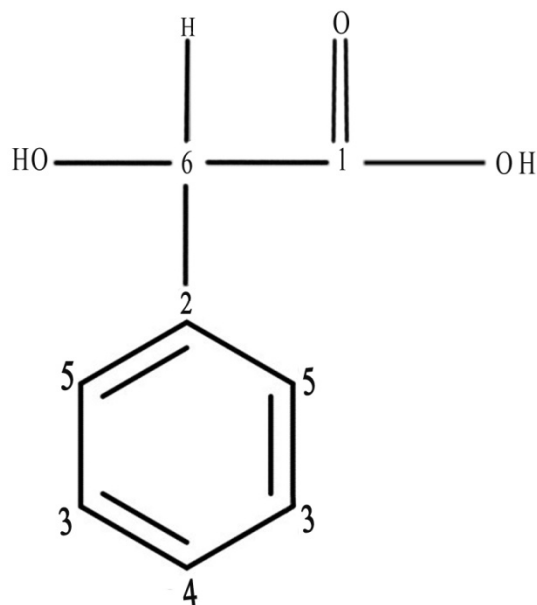


Fig.7 (b). ^{13}C NMR atomic numbering of RMA crystal

In ^{13}C -NMR spectrum, the signal observed at 176.06 ppm corresponds to the carbon 1 of COOH mandelic acid. The peak at 137.86 ppm is due to carbon 2 of group. The signals observed at 129.04 ppm, 129.01 ppm and 127.02 ppm are due to carbon 3, 4 and 5 of CH group. The peak at 72.34 ppm is attributed (carbon 6 group. The observed values matches with the literature values [11].

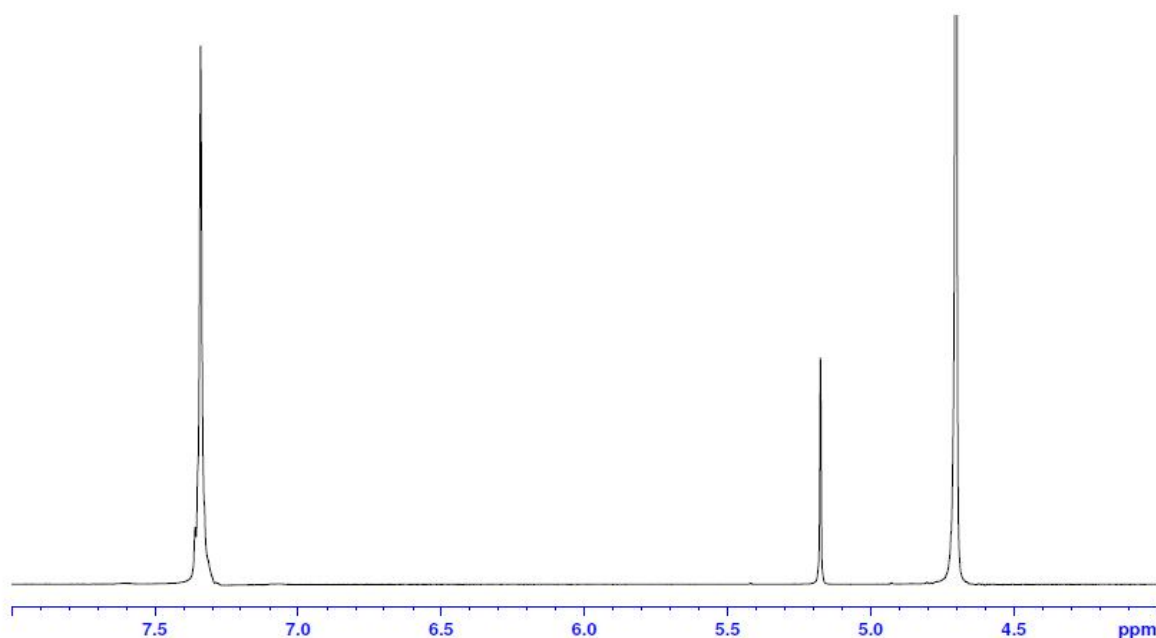


Fig.8 ^1H NMR spectrum of RMA crystal

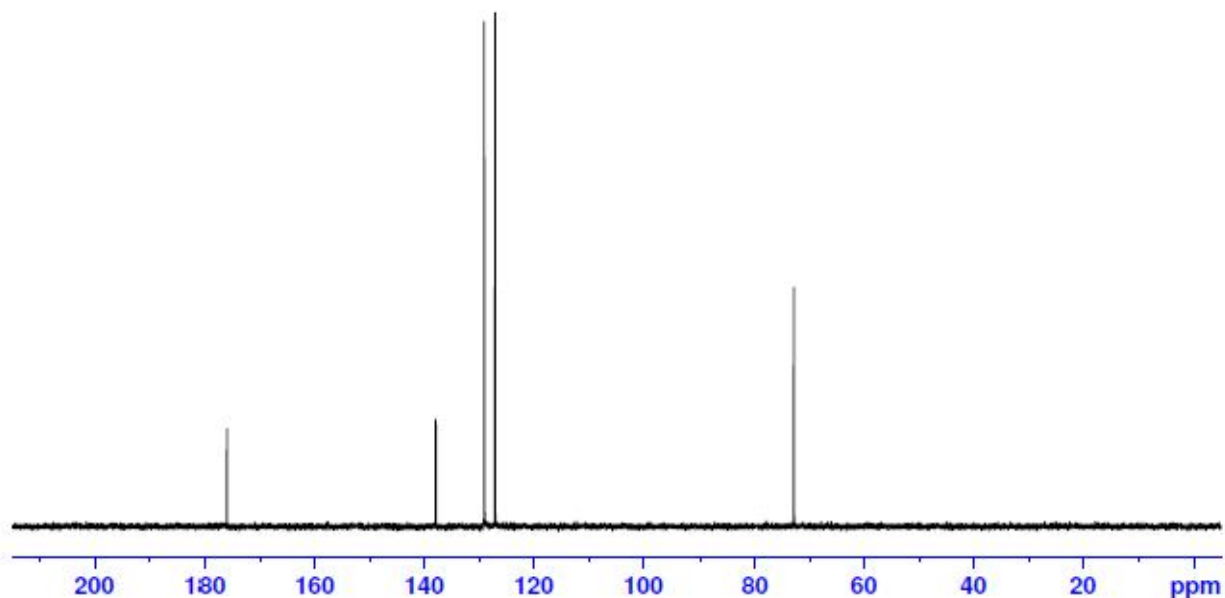
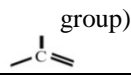
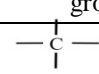


Fig.9 ^{13}C NMR spectrum of RMA crystal

Table 3. Chemical shifts in ^1H NMR and ^{13}C NMR spectra of RMA

Spectra	Chemical shift (ppm)	Group identification
^1H NMR	4.702	D_2O
	5.175	CH proton (1)
	7.359-7.339	CH proton of ring (2)
^{13}C NMR	176.06	Carbon 1 (COOH group)
	137.86	Carbon 2 ( group)
	129.04	Carbon 3 (CH group)
	129.01	Carbon 4 (CH group)
	127.02	Carbon 5 (CH group)
	72.77	Carbon 6 ( group)

H. Second Harmonic Generation Analysis

The SHG property of RMA is measured by the modified version of powder technique by Kurtz and Perry. The fundamental beam of 1064 nm from Q-switched Nd:YAG laser is used to test the RMA crystal. The RMA is grind into fine powder and closely packed in

a micro capillary tube. It was kept in the way of Nd: YAG laser. (Beam energy= 0.701 J/pulse, pulse width= 6 ns, repetition rate = 10 Hz). The NLO output of reference material KDP is 8.91 mJ while that of RMA is 6.39 mJ, which is 0.71 times that of KDP.

I. Z-scan Measurement

The third-order NLO optical property of RMA single crystal was analyzed by Z-scan method. The NL refractive index (n_2), NL absorption coefficient (β) of RMA single crystal was evaluated. In this method, He-Ne laser (632.8 nm) having beam radius 2 mm was used to scan RMA. n_2 was determined by using,

$$n_2 = \frac{\Delta\phi}{KI_0L_{eff}}$$

Where $K = 2\pi / \lambda$, I_0 is the intensity of the laser beam at the focus ($Z=0$), L_{eff} is thickness of the crystal and is given by,

$$L_{eff} = \frac{1 - \exp(-\alpha L)}{\alpha}$$

Here α -represents linear absorption coefficient and $L=1$ mm (thickness of RMA). Closed aperture Z-scan curve was shown in Fig.10. In closed curve, peak followed by valley reveals the negative nonlinear refractive index (n_2) of material. This suggests that crystal having self-defocusing nature.

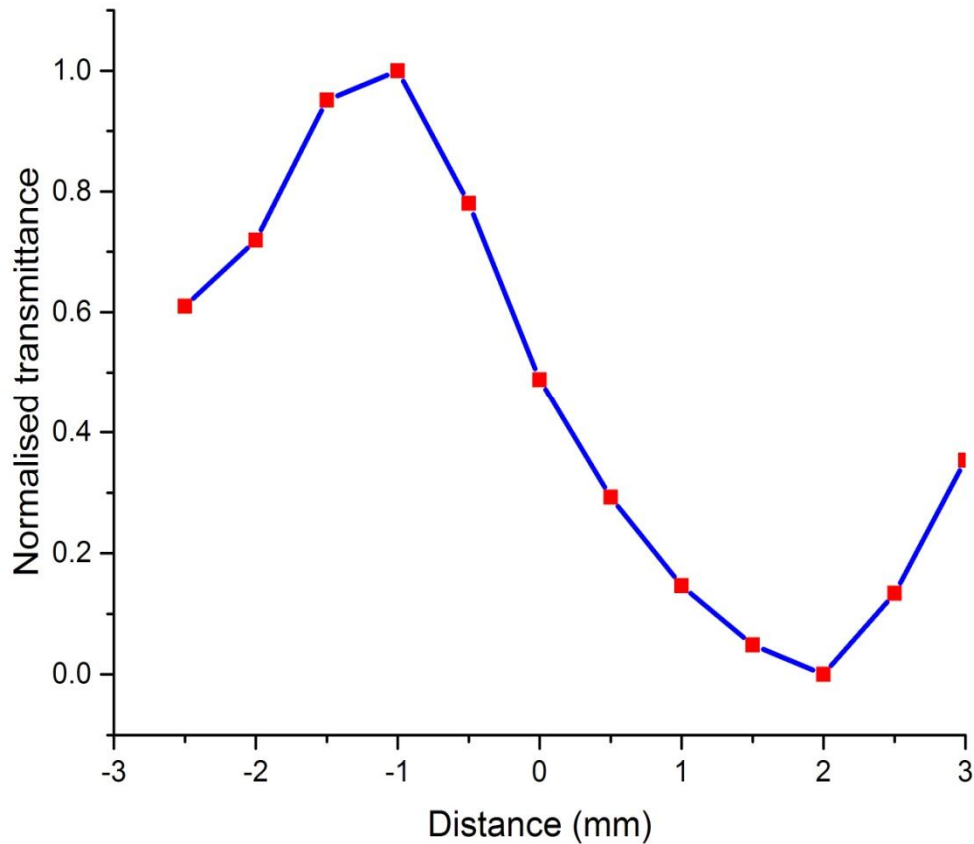


Fig.10 Closed aperture Z-scan pattern of RMA crystal

(β) is estimated using expression,

$$\beta = \frac{2\sqrt{2}\Delta T}{I_0L_{eff}}$$

Where $\Delta T = 1 - T_v$, T_{v-} valley value at the open aperture curve (Fig.11). The maximum transmission occurs near the focus and attributed to saturable absorption of RMA [12].

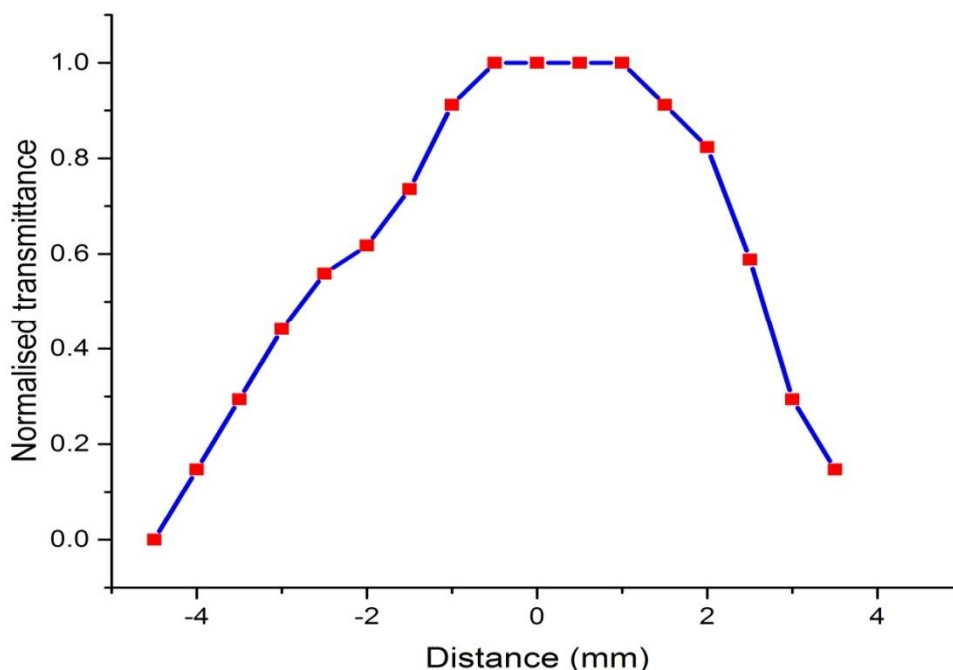


Fig.11 Open aperture Z-scan pattern of RMA crystal

The real and imaginary parts of the third order NLO susceptibility $\chi^{(3)}$ are defined as

$$\text{Re } \chi^{(3)\text{esu}} = 10^{-4} \epsilon_0 C^2 n_0^2 n_2 / \pi \quad (\text{cm}^2 / \text{W}),$$

$$\text{Im } \chi^{(3)\text{esu}} = 10^{-2} \epsilon_0 C^2 n_0^2 \lambda \beta / 4\pi^2 \quad (\text{cm} / \text{W}),$$

Where ϵ_0 = the vacuum permittivity, n_0 is the linear refractive index of the sample and $\chi^{(3)}$ is calculated from

$$C = 3 \times 10^{10} \text{ cm} / \text{sec}$$

$$\chi^3 = \sqrt{[\text{Re}(\chi^3)]^2 + [\text{Im}(\chi^3)]^2}$$

Table 4 presents n_2 , β and χ^3 .

Table 4. Measurement details and the results of the Z- scan technique

Laser beam wavelength (λ)	632.8 nm
Lens focal length (f)	22.5 cm
Optical path distance (Z)	115 cm
Spot-size diameter in front of the aperture (ω_a)	1 cm
Aperture radius (r_a)	2 mm
Incident intensity at the focus (Z=0)	3.13 MW/ cm ²
Nonlinear refractive index (n_2)	- 6.5 x 10 ⁻¹¹ cm ² /W
Nonlinear absorption coefficient (β)	- 4.974 x 10 ⁻⁴ cm/W
Real part of the third-order susceptibility [Re (χ_3)]	-1.28 x 10 ⁻⁷ esu
Imaginary part of the third-order susceptibility [Im (χ_3)]	4.972 x 10 ⁻⁶ esu
Third-order nonlinear optical susceptibility (χ_3)	4.9 x 10 ⁻⁶ esu

IV. CONCLUSION

Single crystals of RMA have been grown from an aqueous solution using solvent evaporation technique. It crystallized in monoclinic structure. The lower cut-off wavelength of RMA is 267 nm. The vibrations of functional groups were analysed by FTIR and FT-Raman spectra. The crystal is thermally stable upto 201°C. The molecular structure of RMA was established using ^1H and ^{13}C NMR techniques. The SHG efficiency of RMA was measured as 6.39 mJ. Third order technique n_2 , β and χ^3 were calculated using Z-scan analysis.

V. ACKNOWLEDGEMENTS

Author C.R acknowledges Council of Scientific and Industrial Research (CSIR), New Delhi for financial aid (scheme no: 03(1301)/13/EMR II). The authors are very grateful to Dr. P.K. Das, Indian Institute of Science, Bangalore (IISc) for measurement of SHG efficiency, SAIF, Indian Institute of technology (IIT), Chennai for single crystal XRD and FT-Raman analysis, National institute of technology (NIT), Trichy for powder XRD and Z-scan studies, Sastra University, Thanjavur for FT- NMR studies and St. Joseph's College, Trichy for FT-IR .

REFERENCES

- [1] A.C. Jennifer, D.L. Michael, M. Brian, et al. Tetrahedron: Asymmetry 15 (2004) 2793
- [2] Y. Asano, T. Yasuda, Y. Tani, et al. Agric. Biol. Chem. 46 (1982) 1183.
- [3] G. de Santis, Z.L. Zhu, W.A. Greenberg, et al. J. Am. Chem. Soc. 124 (2002) 9024.
- [4] D. Brady, A. Beeton, J. Zeevaart, et al. Appl. Microbiol. Biotechnol. 64 (2004) 76.
- [5] K.Z. Yamamoto, K. Oishi, I. Fujimashu, et al. Appl. Environ. Microbiol. 57 (1991) 3028.
- [6] P. Kaul, A. Banerjee, S. Mayilraj, et al. Tetrahedron: Asymmetry 15 (2004) 207
- [7] A. O. Patil, Pennington, W. T. Paul, D.Y. Curtin and C.E. Dykstra, Reactions of Crystalline (I?)-(-) and (S)-(+)-Mandelic Acid with Amines. Crystal Structure and Dipole Moment of (S)-Mandelic Acid. A Method of Determining Absolute Configuration of Chiral Crystals; J. Am. Chem. Soc., 109 (1987) 1529-1535.
- [8] V.V. Ghazaryan, B.A. Zakharov, E.V. Boldyreva and A.M. Petrosyan, L-ethioniniumpicrate Spectrochimica Acta A ;142 (2015) 344 .
- [9] S. Natarajan, N.R. Devi, S.A. Martin Britto Dhas and S. Athimoolam, Growth, thermal and optical studies of a new organic NLO material: L-methionine L-methioninium hydrogen maleate Opto. And Adva. Mat. –Rapid Com.: 4 (2010) 516
- [10] Spectral database for organic compounds (SDBS), http://sdfs.db.aist.go.jp/sdfs/cgi-bin/direct_frame_top.cgi
- [11] P.Y. Bruice, organic chemistry, 6th Edition, Prentice Hall (2010),.
- [12] T.C. Sabari Girisun, S. Dhanuskodi, Linear and nonlinear optical properties of trithiourea zinc sulphate single crystals; J. Cryst. Res. Technol. 44 (2009) 1297-1302.



10.22214/IJRASET



45.98



IMPACT FACTOR:
7.129



IMPACT FACTOR:
7.429



INTERNATIONAL JOURNAL FOR RESEARCH

IN APPLIED SCIENCE & ENGINEERING TECHNOLOGY

Call : 08813907089  (24*7 Support on Whatsapp)